Energy and angular momentum radiated for non-head-on binary black hole collisions

Osvaldo Moreschi
FaMAF, Universidad Nacional de Cordoba, Ciudad Universitaria, (5000) Cordoba, Argentina

Alejandro Perez
Center for Gravitational Physics and Geometry, Penn State University, University Park, Pennsylvania 16802

Luis Lehner
Department of Physics & Astronomy, The University of British Columbia, Vancouver, British Columbia, Canada V6T 1Z1
(Received 9 May 2002; published 25 November 2002)

We investigate the possible total radiated energy produced by a binary black hole system containing non-vanishing total angular momentum. For the scenarios considered we find that the total radiated energy does not exceed 1%. Additionally we explore the gravitational radiation field and the variation of angular momentum in the process. After the formation of the final black hole, the model uses the Robinson-Trautman (RT) spacetimes as background. The evolution of perturbed RT geometries is carried out numerically.

DOI: 10.1103/PhysRevD.66.104017 PACS number(s): 04.25.Dm, 02.60.Cb, 04.30.Db

I. INTRODUCTION

The advent of powerful detectors capable of directly measuring gravitational radiation for the first time has motivated numerous investigations of systems likely to produce gravitational waves of enough intensity which are expected to be observed with these detectors. Among those systems, a prime candidate is that composed by a couple of inspiraling black holes which eventually merge into one releasing considerable amounts of energy via gravitational radiation. Clearly, because of the strong gravitational fields involved in such a process, its complete description requires solving Einstein equations in their full generality which can only be done through numerical methods [1]. Several groups are combining efforts to numerically model such a system [2–7] and although significant progress has been (and is being) made in this direction (see for instance [1]), an accurate and robust implementation is still missing. In the meantime, valuable insight can be gained through approximate models of the system. These models serve both as means to gain a better understanding of the problem and also to provide information that can serve as tests for the numerical simulations, where the lack of known solutions renders the problem of accuracy assessment more involved.

Traditional models are obtained through perturbative approximations where an expansion with respect to some appropriately chosen parameter provides a reduced and manageable system of equations. Naturally, these approaches provide accurate answers only when the perturbative parameter remains small. For instance, the traditional post-Newtonian approximation (see for instance [8,9]), can be safely used when the black holes are far enough and the relative speeds involved are much smaller than 1. However, as the holes come closer, the gravitational fields and relative speeds involved become very large and it is clear that this approximation will fail to give sensible answers. Resumation techniques [10] and/or effective one-body expansions [11] have been proposed to extend the regime of validity of this approach. However, even when the ambiguities proper of these options can be satisfactorily addressed, they will inevitably break in the late stages of the merger, which for the case of black holes lies in the maximum sensitivity window of earth-based detectors [12,13].

Another approximation, known as the *close limit approximation* (CLA) (see for instance [14,15]) assumes the black holes have already merged and the perturbation parameter can be considered to be how non-Schwarzschild (or non-Kerr) the hole is. Since no-hair theorems imply the final fate of the formed black hole should be of the Kerr-type, this approach can safely be used to describe such epoch (note however, that in certain situations, the CLA has been able to produce valuable results at rather earlier times when the holes had just merged; however, it is not clear that this will hold in generic cases).

A different approximate model can be obtained by considering Robinson-Trautman spacetimes [16] which contain purely outgoing gravitational radiation and decay to leave a Schwarzschild-like horizon [17–19]. These spacetimes are thus natural candidates to study systems settling to a single black hole. The idea here would be to use them as background spacetimes for a perturbation treatment.[1] For instance, a perturbation approach can be constructed where the perturbation parameter is the gravitational radiation produced by the system [20]. This indeed appears as an enticing suggestion since the system is not expected to produce total radiation outputs in excess of a few percent of the initial mass.

In the past, this idea was pursued to produce estimates of the total gravitational radiation [21,22] obtaining excellent agreement with numerical relativity results for the head-on collision, i.e. zero angular momentum case [23]. These studies did not allow for the spacetime to have total angular momentum and also the physical situations considered pro-

[1]Note that this approach would therefore have a background spacetime which radiates as opposed to considering perturbations off a stationary spacetime.

duced small enough radiation output that the equations governing the dynamic of the perturbations were solved in the asymptotic late-time linear regime [21,22].

In order to consider more interesting scenarios, perturbations allowing for angular momentum were introduced in [24] thus paving the way for studies of more generic situations. In the present work, we perform such studies by numerically solving the dynamical equations introduced in [24] in their full generality. Our studies are aimed towards obtaining a deeper understanding of the system and also with the hope of producing information that can be used as a check of full numerical relativistic simulations.

This work is organized as follows. In Sec. II we briefly review the perturbative treatment of Robinson-Trautman (RT) spacetimes that allows for angular momentum. Section III describes the physical parameters and how to make the matching between the two eras that appear in our model. The numerical implementation to solve the equations that govern the evolution of the perturbations is described in Sec. IV. The numerical results are presented in Sec. V where the total energy, the gravitational radiation field and the evolution of angular momentum are shown. We conclude with some final comments in Sec. VI.

II. GENERAL ANGULAR MOMENTUM PERTURBATIONS OF RT SPACETIMES

In [24], generic perturbations of RT spacetimes, which include angular momentum, have been presented.

It is convenient to express the geometry in terms of a null tetrad (ℓ^a, m^a, $\overline{m}^a$, n^a) where

$$g_{ab}\ell^a n^b = -g_{ab}m^a\overline{m}^b = 1 \tag{1}$$

with all other possible scalar products being zero; then, the metric can be expressed by

$$g_{ab} = \ell_a n_b + n_a \ell_b - m_a\overline{m}_b - \overline{m}_a m_b . \tag{2}$$

In terms of the coordinate system $(x^0,x^1,x^2,x^3)=(u,r,(\zeta+\overline{\zeta}),(1/i)(\zeta-\overline{\zeta}))$, where u is a null coordinate and r is an affine parameter along the geodesic integral lines of the vector ℓ^a, one can express the null tetrad in terms of its components by the relations:

$$\ell_a = (du)_a \tag{3}$$

$$\ell^a = \left(\frac{\partial}{\partial r}\right)^a \tag{4}$$

$$m^a = \xi^i\left(\frac{\partial}{\partial x^i}\right)^a \tag{5}$$

$$\overline{m}^a = \overline{\xi^i}\left(\frac{\partial}{\partial x^i}\right)^a \tag{6}$$

$$n^a = U\left(\frac{\partial}{\partial r}\right)^a + X^i\left(\frac{\partial}{\partial x^i}\right)^a \tag{7}$$

with $i=0,2,3$ and $\zeta=\frac{1}{2}(x^2+ix^3)$; and where the components ξ^i, U and X^i are given by the following expressions:

$$\xi^0 = 0,$$

$$\xi^2 = \frac{\xi_0^2}{r} + \lambda\,\overline{\xi_0^2}\left(-\frac{\sigma_0}{r^2} + \frac{1}{r}\frac{\partial^2 W_0}{\partial r^2} - \frac{2}{r^2}\frac{\partial W_0}{\partial r}\right), \tag{8}$$

$$\xi^3 = \frac{\xi_0^3}{r} + \lambda\,\overline{\xi_0^3}\left(-\frac{\sigma_0}{r^2} + \frac{1}{r}\frac{\partial^2 W_0}{\partial r^2} - \frac{2}{r^2}\frac{\partial W_0}{\partial r}\right)$$

$$\xi_0^2 = \sqrt{2}P_0 V, \quad \xi_0^3 = -i\,\xi_0^2; \tag{9}$$

$$U = rU_{00} + U_0 + \frac{U_1}{r} + \frac{U_2}{r^2} + \Delta U_3, \tag{10}$$

$$U_{00} = \frac{\dot{V}}{V},$$

$$U_0 = -\frac{1}{2}K_V,$$

$$U_1 = -\frac{1}{2}(\Psi_2^0 + \overline{\Psi}_2^0), \tag{11}$$

$$U_2 = \frac{\lambda}{6}(\eth_{V_{RT}}\overline{\Psi}_1^0 + \overline{\eth}_{V_{RT}}\Psi_1^0),$$

$$\Delta U_3 = -\frac{\lambda}{r^2}(\overline{\eth}^2_{V_{RT}}W_0 + \eth^2_{V_{RT}}\overline{W}_0);$$

$$X^0 = 1,$$

$$X^2 = \lambda\,\xi_0^2\left(-\frac{\overline{\tau}_0}{r^2} + \frac{2\overline{\Psi}_1^0}{3r^3} + \frac{2}{r^2}\frac{\partial\eth_{V_{RT}}\overline{W}_0}{\partial r} - \frac{4}{r^3}\eth_{V_{RT}}\overline{W}_0\right) + \text{c.c.}, \tag{12}$$

$$X^3 = \lambda\,\xi_0^3\left(-\frac{\overline{\tau}_0}{r^2} + \frac{2\overline{\Psi}_1^0}{3r^3} + \frac{2}{r^2}\frac{\partial\eth_{V_{RT}}\overline{W}_0}{\partial r} - \frac{4}{r^3}\eth_{V_{RT}}\overline{W}_0\right) + \text{c.c.},$$

where

$$\tau_0 = \overline{\eth}_{V_{RT}}\sigma_0, \tag{13}$$

c.c. means complex conjugate,

$$K_V = \frac{2}{V}\overline{\eth}_V\eth_V V - \frac{2}{V^2}\eth_V V\ \ \overline{\eth}_V V + V^2, \tag{14}$$

and where in these equations we are explicitly denoting the first order terms by introducing the first order parameter λ

dependency, and where $\eth_V$ is the edth operator [25–27], in the GHP notation [28], of the sphere with metric

$$dS^2=\frac{1}{P^2}d\zeta d\overline{\zeta}, \tag{15}$$

where $P=V(u,\zeta,\overline{\zeta})P_0(\zeta,\overline{\zeta})$, and P_0 is the value of P for the unit sphere.

The scalar V is given by

$$V=V_{RT}+\lambda V_\lambda , \tag{16}$$

where V_{RT} is the RT scalar satisfying the Robinson-Trautman equation

$$-3M_0\dot{V}_{RT}=V_{RT}^4 \ \eth^2\overline{\eth}^2 \ V_{RT}-V_{RT}^3 \ \eth^2 V_{RT} \ \overline{\eth}^2 V_{RT}, \tag{17}$$

V_λ is the linear perturbation scalar and $\eth$ is the edth operator of the unit sphere. One can then express K_V by

$$K_V=K_{V_{RT}}+\lambda \ K_{V_\lambda}, \tag{18}$$

where

$$K_{V_{RT}}=\frac{2}{V_{RT}}\overline{\eth}_{V_{RT}}\eth_{V_{RT}}V_{RT}-\frac{2}{V_{RT}^2}\eth_{V_{RT}}V_{RT} \ \overline{\eth}_{V_{RT}}V_{RT}+V_{RT}^2, \tag{19}$$

and

$$\begin{aligned}K_{V_\lambda}=&\frac{2}{V_{RT}}\overline{\eth}_{V_{RT}}\eth_{V_{RT}}V_\lambda-\frac{2}{V_{RT}^2}\eth_{V_{RT}}V_\lambda \ \overline{\eth}_{V_{RT}}V_{RT}\\&-\frac{2}{V_{RT}^2}\eth_{V_{RT}}V_{RT} \ \overline{\eth}_{V_{RT}}V_\lambda+\frac{2V_\lambda}{V_{RT}^3}\eth_{V_{RT}}V_{RT} \ \overline{\eth}_{V_{RT}}V_{RT}\\&+V_\lambda V_{RT}+\frac{V_\lambda}{V_{RT}}K_{V_{RT}}.\end{aligned} \tag{20}$$

In the above equations we have $\sigma_0=\sigma_0(u,\zeta,\overline{\zeta})$, $W_0=W_0(u,r,\zeta,\overline{\zeta})$, $\Psi_1^0=\Psi_1^0(u,\zeta,\overline{\zeta})$ and

$$\Psi_2^0=\Psi_2^0(u,\zeta,\overline{\zeta})=-(M_0+\lambda[M_1(u,\zeta,\overline{\zeta})+i\,\mu(u,\zeta,\overline{\zeta})]); \tag{21}$$

where μ is related to σ_0 by

$$\mu=\frac{1}{2i}(\eth_{V_{RT}}^2\overline{\sigma}_0-\overline{\eth}_{V_{RT}}^2\sigma_0). \tag{22}$$

In order to study the intrinsic fields at future null infinity (scri), it is convenient to consider the leading order behavior of W_0, namely

$$W_0=\frac{\Psi_0^0}{4!r}+W_1, \tag{23}$$

where $\Psi_0^0=\Psi_0^0(u,\zeta\cdot\overline{\zeta})$ and $W_1=O(1/r^2)$. It is interesting to note that the component $\Psi_0=\partial^4W_0/\partial r^4$ of the Weyl tensor is given in this case [24] by

$$\Psi_0=\frac{\Psi_0^0}{r^5}+\frac{\partial^4W_1}{\partial r^4}, \tag{24}$$

where the second term is of order $O(1/r^6)$.

The remaining equations at scri are

$$\dot{\Psi}_0^0=3\frac{\dot{V}_{RT}}{V_{RT}}\Psi_0^0+\eth_{V_{RT}}\Psi_1^0-3M_0\sigma_0, \tag{25}$$

$$\dot{\Psi}_1^0=3\frac{\dot{V}_{RT}}{V_{RT}}\Psi_1^0-\eth_{V_{RT}}(M_1+i\mu)-\overline{\eth}_{V_{RT}}(K_{V_{RT}})\sigma_0 \tag{26}$$

and

$$\begin{aligned}-6M_0\frac{\dot{V}_\lambda}{V_{RT}}=&\overline{\eth}_{V_{RT}}\eth_{V_{RT}} \ K_{V_\lambda}-6\frac{\dot{V}_{RT}}{V_{RT}}\left(3M\frac{V_\lambda}{V_{RT}}-M_1\right)-2\dot{M}_1\\&-\frac{\dot{V}_{RT}}{V_{RT}}\overline{\eth}_{V_{RT}}^2\sigma_0+2\frac{\dot{V}_{RT}}{V_{RT}^2}\overline{\eth}_{V_{RT}}V_{RT}\overline{\eth}_{V_{RT}}\sigma_0\\&-\frac{2}{V_{RT}}\overline{\eth}_{V_{RT}}\dot{V}_{RT}\overline{\eth}_{V_{RT}}\sigma_0+\overline{\eth}_{V_{RT}}^2\dot{\sigma}^0-\frac{\dot{V}_{RT}}{V_{RT}}\eth_{V_{RT}}^2\overline{\sigma}_0\\&+2\frac{\dot{V}_{RT}}{V_{RT}^2}\eth_{V_{RT}}V_{RT}\eth_{V_{RT}}\overline{\sigma}_0\\&-\frac{2}{V_{RT}}\eth_{V_{RT}}\dot{V}_{RT}\eth_{V_{RT}}\overline{\sigma}_0+\eth_{V_{RT}}^2\dot{\overline{\sigma}}^0.\end{aligned} \tag{27}$$

The objective is to use the solutions of the previous equations to model a black hole that just formed after the non-head-on collision of a previous binary system. In this model the idea is to only make use of the information of the individual masses and the total angular momentum. With all this in mind we have to chose the appropriate gauge and free functions.

In Ref. [24] it was discussed the gauge freedom of these spacetimes. In order not to introduce extra structure, we will chose the free functions and gauges that make

$$M_1=0 \tag{28}$$

and

$$\sigma_0=0. \tag{29}$$

Other choices will force extra structure on the model beyond masses and angular momentum, as mentioned above.

With this choice the previous equations become

$$\dot{\Psi}_0^0=3\frac{\dot{V}_{RT}}{V_{RT}}\Psi_0^0+\eth_{V_{RT}}\Psi_1^0, \tag{30}$$

$$\dot{\Psi}_1^0 = 3\frac{\dot{V}_{RT}}{V_{RT}}\Psi_1^0 \tag{31}$$

and

$$-6M_0\dot{V}_\lambda = V_{RT}\bar{\eth}_{V_{RT}}\eth_{V_{RT}}\ K_{V_\lambda} - 18M_0\dot{V}_{RT}\left(\frac{V_\lambda}{V_{RT}}\right). \tag{32}$$

It is interesting to note that since the RT equation can also be expressed as

$$-6M_0\frac{\dot{V}_{RT}}{V_{RT}} = \bar{\eth}_{V_{RT}}\eth_{V_{RT}}K_{V_{RT}}, \tag{33}$$

Eq. (32) can be written in the following way:

$$-6M_0\,\dot{V}_\lambda = V_{RT}\bar{\eth}_{V_{RT}}\eth_{V_{RT}}\ K_{V_\lambda} + 3V_\lambda\bar{\eth}_{V_{RT}}\eth_{V_{RT}}K_{V_{RT}}. \tag{34}$$

Given initial conditions for the functions V_{RT}, Ψ_0^0, Ψ_1^0 and V_λ Eqs. (17), (30), (31) and (32) provide for the respective evolutions.

The radiation content of the spacetime is easily described by the time derivative of the Bondi shear. Let σ_B^0 denote the Bondi shear and u_B the Bondi time; then for any section of scri $u=$const one can express the radiation content from the relation [29]

$$\frac{\partial\sigma_B^0}{\partial u_B} = \frac{\eth^2 V}{V}; \tag{35}$$

therefore to first order one has

$$\frac{\partial\sigma_B^0}{\partial u_B} = \frac{\eth^2 V_{RT}}{V_{RT}} + \lambda\left(\frac{\eth^2 V_\lambda}{V_{RT}} - \frac{V_\lambda\eth^2 V_{RT}}{V_{RT}^2}\right). \tag{36}$$

The radiation flux at the retarded time u is given by

$$F_B(u) = \frac{1}{4\pi}\int_{S_u}\frac{\partial\sigma_B^0}{\partial u_B}\frac{\partial\bar{\sigma}_B^0}{\partial u_B}dS^2. \tag{37}$$

Let us recall that in this case the timelike component of the Bondi momentum at the section $u=$const can be calculated from

$$P_B^0 = \frac{1}{4\pi}\int\ \frac{M_0}{V^3}dS^2. \tag{38}$$

At the retarded time u, we say that V represents a quadrupole excitation along the y axis if

$$V = 1 + AY_{2,0}(\zeta',\bar{\zeta}'), \tag{39}$$

where A is the amplitude of the excitation, $Y_{2,0}$ is a spherical harmonic, and $(\zeta',\bar{\zeta}')$ are the coordinates of the sphere where the pole is along the y axis. Then in terms of the usual spherical harmonics with coordinates $(\zeta,\bar{\zeta})$, one has

$$V = 1 - \frac{A}{2}\left(\sqrt{\frac{3}{2}}Y_{2,-2}(\zeta,\bar{\zeta}) + Y_{2,0}(\zeta,\bar{\zeta}) + \sqrt{\frac{3}{2}}Y_{2,2}(\zeta,\bar{\zeta})\right). \tag{40}$$

III. FIXING THE PARAMETERS AND THE NEWTONIAN MATCHING

The physical system can be characterized by two stages. During the first stage two black holes are moving towards each other with some orbital angular momentum. At some moment they collide and form a single black hole, which settles down in the asymptotic future to a stationary Kerr geometry.

During the first stage of evolution we describe the gravitational radiation with the quadrupole formula, where the dynamics is worked out from the Newtonian framework. The whole motion is contained in a plane; therefore two variables are sufficient to describe the orbits. The two integrals of motion, namely energy E and angular momentum j, allow to solve the Newtonian system.

The initial data are assumed to be given in the (x,y) plane, with zero total momentum and such that the orbital angular momentum is along the positive $\hat{z}$ direction.

The initial velocities can be thought to have components along the x axis only. Let us call R_0 the initial impact parameter, at some initial relative distance r_0. In this way, using the relative velocity v_0, one has

$$E = \frac{\mu}{2}v_0^2 - \frac{Gm_1m_2}{r_0}, \tag{41}$$

$$j = \mu R_0 v_0, \tag{42}$$

where $\mu = m_1m_2/(m_1+m_2)$ is the reduced mass.

For this kind of motion the quadrupole formula predicts that the power of gravitational radiation is given by

$$F_Q(r) = \frac{8}{15}(Gm_1m_2)^2\left[\frac{2}{\mu r^4}\left(E + \frac{Gm_1m_2}{r}\right) + \frac{11j^2}{\mu^2r^6}\right], \tag{43}$$

which generalizes the analog equation appearing in Ref. [22].

In order to continue the dynamical description after the collision of the two black holes, we need to have a merging condition in the Newtonian framework. In Refs. [21] and [22] we have succeeded in estimating the total energy radiated in the head-on black hole collision using the following criteria. When a black hole, which mass at infinity is m_{i1}, is brought to a distance r_{12} of another black hole of asymptotic mass m_{i2}, its physical mass, for the stationary situation, is changed [30] to

$$m1 = m_{i1} + \frac{m_{i1}m_{i2}}{2r_{12}}, \tag{44}$$

and similarly for the other mass.

Applying the arguments of Ref. [22] one concludes that the merging condition should be taken when the separation distance has the value

$$r_c=2(m1+m2). \tag{45}$$

It is convenient to introduce the relative mass parameter α and the reference mass m, so that $m_{i1}=m$ and $m_{i2}=\alpha m$. Then the merging condition [22] gives

$$r_c=(m_{i1}+m_{i2})\left[1+\sqrt{1+\frac{2\alpha}{(1+\alpha)^2}}\right]. \tag{46}$$

Let us now consider the initial data used in Ref. [2] for the grazing collisions of black holes; namely: $x_1=5m$, $x_2=-5m$, $y_1=m$, $y_2=-m$, $v_{x1}=-0.5$ and $v_{x2}=0.5$, with $m=1$ and $\alpha=1$. These data correspond to a hyperbolic Newtonian trajectory, with initial separation distance $r=10.198$, and critical merging radius $r_c=4.449$.

Our strategy is to follow closely the model used in [21,22]; but we also want to compare our work with [2]. However, the initial data of [2] involve two black holes with half the speed of light each; therefore in adapting this initial data to our model we must take into account relativistic effects. In Refs. [21] and [22] there was no need for these concerns because the initial data were not relativistic.

Since the initial velocities are relativistic, the relative initial velocity v_0 is calculated from the expression

$$v_0=\frac{v_{x2}-v_{x1}}{1-v_{x1}v_{x2}}=0.8, \tag{47}$$

where we are using geometric units in which the velocity of light and the gravitational constant have the unit value.

The energy radiated during the falling phase, calculated from Eq. (43) is $E_N=0.00346(m_1+m_2)$.

In order to match the Newtonian stage with the black hole RT perturbed model we need also to set the total initial mass and initial angular momentum for the RT stage.

In previous work we have matched the Newtonian mass $M_{New}=m_{i1}+m_{i2}$ to the initial mass M; this already takes into account the field relativistic first order correction in terms of its physical masses $m1$ and $m2$, since, recalling Eq. (21) of Ref. [22], the initial mass would be $m1+m2-m_{i1}m_{i2}/r_{12}$. The system discussed in Ref. [22] had zero initial velocity, and therefore there was no need to take into account any other effect. Instead in our case we should take into account speed relativistic corrections.

Then, since the initial data are relativistic, the initial mass and angular momentum are calculated from

$$M=\frac{m_{i1}}{\sqrt{1-v_1^2}}+\frac{m_{i2}}{\sqrt{1-v_2^2}}=2.309 \tag{48}$$

and

$$J=-y_1\frac{m_{i1}v_{x1}}{\sqrt{1-v_{x1}^2}}-y_2\frac{m_{i2}v_{x2}}{\sqrt{1-v_{x2}^2}}=1.155. \tag{49}$$

It should be emphasized that the relation between the initial RT stage mass and angular momentum M and J with the Newtonian mass and angular momentum M_{New} and j is just the Lorentzian factor $\gamma=1/\sqrt{1-v_{x1}^2}=1.1547$. In the last section we will comment on the incidence of this factor on our results.

Let us observe that the relation between the relativistic angular momentum and total mass is $J/M^2=0.217$.

Since the angular momentum is small, it can be treated as a perturbation. At the moment of the collapse, we can consider a quadrupole excitation along the y axis with amplitude A, as described above. Let us take $A=A_m+A_j$, where A_j is the contribution coming from the appearance of the angular momentum j. The matching condition is given by the equation [see Eqs. (35), (37) and (43)]

$$F_B=F_Q(r_c), \tag{50}$$

from which one obtains in this case

$$A_m=0.057 \tag{51}$$

and

$$A_j=0.028. \tag{52}$$

Therefore, to be explicit, the initial data for V_{RT} and V_λ are

$$V_{RT}=1-\frac{A_m}{2}\times\left(\sqrt{\frac{3}{2}}Y_{2,-2}(\zeta,\bar{\zeta})+Y_{2,0}(\zeta,\bar{\zeta})+\sqrt{\frac{3}{2}}Y_{2,2}(\zeta,\bar{\zeta})\right) \tag{53}$$

and

$$\lambda V_\lambda=-\frac{A_j}{2}\times\left(\sqrt{\frac{3}{2}}Y_{2,-2}(\zeta,\bar{\zeta})+Y_{2,0}(\zeta,\bar{\zeta})+\sqrt{\frac{3}{2}}Y_{2,2}(\zeta,\bar{\zeta})\right). \tag{54}$$

The constant M_0 is determined from Eq. (38), and the condition that initially the mass is given by Eq. (48), which sets $M_0=2.302$.

The orbital angular momentum is taken into account in the initial data for Ψ_1^0. It is convenient to express these initial data in terms of the auxiliary field g, given by

$$\Psi_1^0=i\frac{\eth_{V_{RT}}g}{V_{RT}^2}=i\frac{\eth g}{V_{RT}}. \tag{55}$$

Let us note that then

$$\eth_{V_{RT}}\Psi_1^0=\eth^2 g$$

so that in the stationary case one has $\eth^2 g=0$ and $\dot{g}=0$.

We take $g=\bar{g}$ and

$$g=g_0Y_{1,0}(\zeta,\bar{\zeta}), \tag{56}$$

where g_0 is related to the angular momentum in the z direction by

$$g_0 = -\sqrt{12\pi}J = -4.094. \tag{57}$$

In Ref. [31] it was also considered a similar case of a binary system with orbital angular momentum. Their initial data were $x_1 = 0$, $x_2 = 0$, $y_1 = m$, $y_2 = -m$, $v_{x1} = -0.8$ and $v_{x2} = 0.894$, with $m = 1.5$ and $\alpha = \frac{2}{3}$. From the Newtonian point of view this data correspond to an elliptic motion, but with maximum and minimum radius that are smaller than the corresponding critical merging radius. For this reason, we cannot compare this case with our model.

IV. NUMERICAL IMPLEMENTATION

Accurate numerical evolution of a fourth order parabolic equation, such as Eq. (17), by means of an explicit finite difference scheme is a challenge because the Courant-Friedrich-Lewy (CFL) [32] condition requires that the time step Δu scale as the fourth power of the spatial grid size. Nevertheless, we constructed a set of algorithms to solve these equations using second order accurate finite difference approximations (following [33]). The numerical treatment of the *eth* operator has been thoroughly described in [33]. This work presented a clean way to deal with derivative operators on the sphere by covering it with two coordinate patches and dealing with spin weighted quantities. Thus, it is ideally suited for our present purposes. The numerical grid on each patch is defined by $\xi_{ij} = q_i + i p_j$ where $q_i, p_i = -1 - 2\Delta_A + (i-1)\Delta_A$ [with $\Delta_A = 2/(N_A - 5)$]. The angular derivatives are discretized by centered second order finite difference approximations and information between patches is obtained through fourth order accurate interpolations. (For a detailed description of this approach see [33].)

The integration in time is based upon a three time level Adams-Bashford [32] scheme with predictor ($\tilde{\mathcal{F}}$) given by

$$\tilde{\mathcal{F}}(u+\Delta u) = \mathcal{F}(u) + \frac{\Delta u}{2}\partial_u[3\mathcal{F}(u) - \mathcal{F}(u-\Delta u)], \tag{58}$$

and corrector

$$\mathcal{F}(u+\Delta u) = \mathcal{F}(u) + \frac{\Delta u}{2}\partial_u[\mathcal{F}(u) + \tilde{\mathcal{F}}(u+\Delta u)] + O(\Delta u^3), \tag{59}$$

where $\mathcal{F}$ stands for V_{RT} or V_λ and the ∂_u terms are to right hand sides of Eqs. (27). Additionally, we implemented the iterative Cranck-Nicholson algorithm [34,35] and observed that the results obtained with both implementations agree. Since the evolution equation for Ψ_0^0 is linear, its numerical integration is straightforwardly done by centered second order differences at the level $(u + \Delta u/2)$.

The second order convergence of numerical solutions was confirmed in the perturbative regime using solutions of the linearized equation and second order self-convergence of the solutions was confirmed in the nonlinear regime.

V. RESULTS

A. Variations of total energy

The total Bondi energy-momentum vector at any RT retarded time u can be calculated from the expression

$$P^a = -\frac{1}{4\pi}\int_S l^a(\zeta,\bar{\zeta})(\Psi_{B2}^0 + \sigma_B \dot{\bar{\sigma}}_B)\, dS^2, \tag{60}$$

where S is the section determined by $u = \text{const}$,

$$(l^a) = \left(1, \frac{\zeta+\bar{\zeta}}{1+\zeta\bar{\zeta}}, \frac{\zeta-\bar{\zeta}}{i\left(1+\zeta\bar{\zeta}\right)}, \frac{\zeta\bar{\zeta}-1}{1+\zeta\bar{\zeta}}\right), \tag{61}$$

and the subscript B is used to emphasize that the quantities are evaluated with respect to a Bondi frame. The mass M at this section S is then given by

$$M = \sqrt{P^a P_a}, \tag{62}$$

where the indices are raised and lowered by the Lorentzian flat metric η_{ab} at scri [36].

Let us note that the relations between the Bondi quantities and the intrinsic ones are

$$\Psi_{B2}^0 = \frac{\Psi_2^0}{V^3} \tag{63}$$

and

$$\sigma_B = \frac{\sigma}{V}; \tag{64}$$

therefore in our gauge one has $\sigma_B = 0$, at each RT section.

The gravitational energy radiation flux is calculated from the Bondi time derivative of the supermomentum Ψ [37]; namely

$$\frac{\partial \Psi}{\partial u_B} = \frac{\partial \sigma_B}{\partial u_B}\frac{\partial \bar{\sigma}_B}{\partial u_B}. \tag{65}$$

If one instead considers the time change with respect to the RT time, it is convenient to have in mind that for any function f one has

$$\frac{\partial f}{\partial u_B} = \frac{1}{V}\frac{\partial f}{\partial u}. \tag{66}$$

The so called news function $\partial \sigma_B / \partial u_B$ can be expressed in terms of the perturbed RT fields by

$$\frac{\partial \sigma_B}{\partial u_B} = \frac{\eth^2 V}{V} + \frac{1}{V^2}\left(\dot{\sigma} - \frac{\dot{V}}{V}\sigma\right). \tag{67}$$

To calculate the total energy radiated, one could then numerically evaluate the gravitational energy radiation flux of Eq. (65) at different times and sum along all the elapsed time. However, it is more accurate to numerically evaluate the initial mass and subtract the final mass. This is due to the

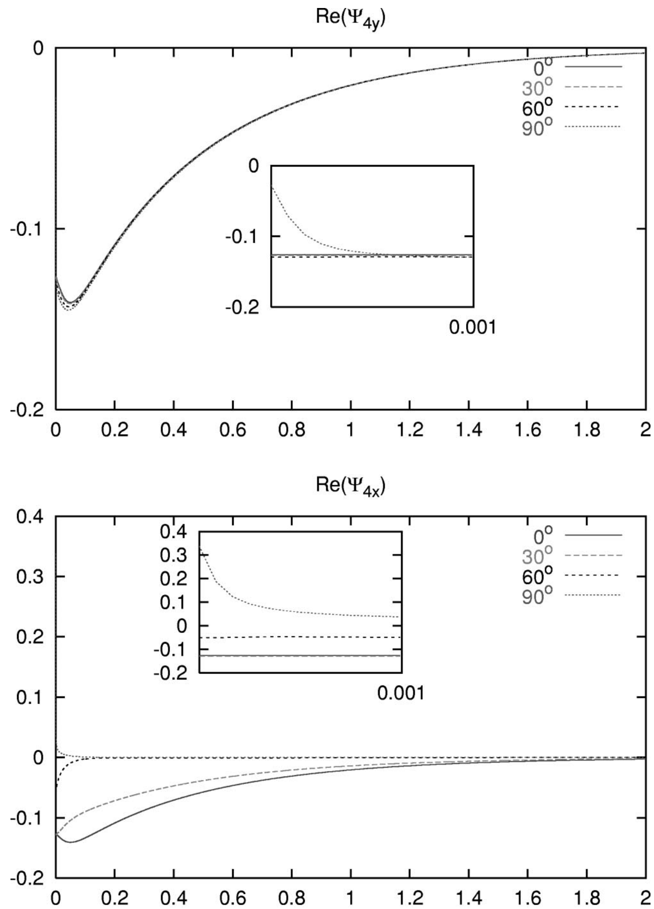

FIG. 1. Evolution of Ψ_4 as a function of time. The subscript x and y refer to the x and y axis of the stereographic coordinate $\zeta = x + iy$ of the northern hemisphere. Each of the four curves refer to detectors at 0°, 30°, 60° and 90°, measured from the north pole of the sphere. The insets show the detail of the rapid time variations at the beginning.

fact that the RT spacetime is known to converge asymptotically to the Schwarzschild one; more specifically, one knows that $\lim_{u\to\infty} V_{RT} = 1$, and similarly one can see that $\lim_{u\to\infty} V_\lambda = 0$.

Using this procedure, and a resolution of $n = 32$ points for half a meridian of the sphere (approximately $N = 1600$ points for the whole sphere), the energy radiated E_{RT} during the RT stage is found to be $E_{RT} = 0.0034 M_0$.

Then, since in units of M_0, the energy radiated in the first stage is $E_N = 0.0030 M_0$, the total energy radiated in the whole process is $E = 0.0064 M_0$.

B. Gravitational radiation field

The numerical calculation of the evolution of the gravitational radiation field Ψ_4, is shown in Fig. 1.

It can be seen that although the total energy radiated is rather small, the amplitude of the gravitational radiation field can be large. In other words, this model describes a noticeable burst.

This is interesting since Ψ_4 is precisely what gravitational wave detectors will measure.

C. Variations of angular momentum

When dealing with the notion of angular momentum one is faced with the fact that there are several inequivalent definitions of angular momentum, which are not tightly related with the notion of intrinsic angular momentum, with the exception of [38]. An appropriate definition of intrinsic angular momentum involves the selection of unique sections [38] of future null infinity where the quantity is to be calculated. Since in our case we are taking the angular momentum as a perturbation parameter of the RT geometries, it is not essential to consider these refinements in our model. And also, since the RT spacetimes provide with a geometric unique family of sections of future null infinity, namely the sections $u = \text{const}$, it is natural to use them to calculate the angular momentum.

Then, instead of describing the variation of the intrinsic angular momentum we describe the variation of the RT-angular momentum vector given by

$$J^k = \Re\mathrm{e}\left[\int_{S_{RT}} \frac{i}{4\pi} \bar{\eth} \ell^k \Psi^0_{B1} dS_B^2 \right], \tag{68}$$

where S_{RT} are the sections determined by $u = \text{const}$, $k = 1,2,3$, so that ℓ^k are the spacelike components of ℓ^a; and where the Bondi component Ψ^0_{B1}, of the Weyl tensor, is related to the RT Weyl component Ψ^0_1 by

$$\Psi^0_{B1} = \frac{\Psi^0_1}{V^3}. \tag{69}$$

Figure 2 shows a very small and smooth variation of the angular momentum; which is more related to the time variation of the RT geometry than to the radiation of angular momentum, as can be seen from the nature of Eq. (31).

VI. FINAL COMMENTS

The estimate of the total gravitational energy radiated in the non-head-on collision of two black holes is less than one percent according to our model. This is on the low end value of existing numerical results (which are still being refined) and comparable with those obtained with the close limit approximation [39]. It is however worth mentioning that our calculations predict an amplitude of the gravitational waves that could be important from the observational point of view. Additionally, it predicts a rather narrow time duration of the "burst." Since the frequency at which this happens, its amplitude and the time duration can be used as preliminary information for constructing data analysis "filters" [40,41], knowledge of these is of importance while templates from full numerical simulations are not available. We will carry out a detailed study of these in the future.

At first sight there is too large a difference between the numerical results in [2] and the estimates obtained here. However, one should keep in mind several points which (by themselves) can account for this difference. Comments are in place for both the results in [2] and those presented here:

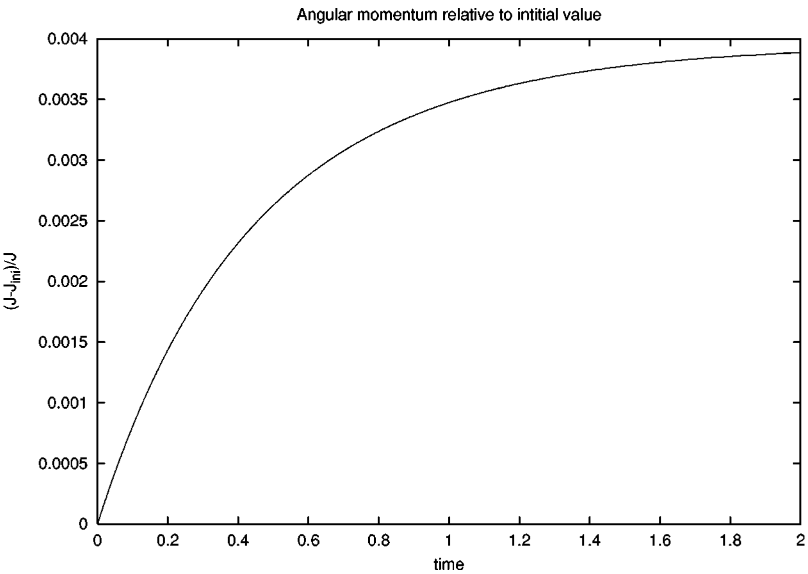

FIG. 2. Evolution of the relative variation of angular momentum J as a function of time.

First, the results in [2] were obtained under a rather coarse resolution and the final numbers need to be refined (there are intense efforts worldwide in this direction). Additionally, the obtained value of radiated energy come from comparissons of initial Arnowitt-Deser-Misner mass and apparent horizon masses. Masses obtained from apparent horizon calculations, in dynamical regimes, are only an approximation of the mass the black hole and hence results obtained through this method can have a significant systematic error. Furthermore it is important to remember that the initial data of [2] is given at a spacelike hypersurface of the spacetime; while, by the nature of the RT spacetime, our initial data is given on a characteristic surface. This implies an essential difference since in the spacelike hypersurface initial data one has incoming and outgoing radiation contributing to the total energy radiated, while in the RT characteristic problem that we solve, we do not consider any incoming initial radiation in our calculations. So, for the relativistic regime, one expects the time slice initial data to radiate more energy than the characteristic case.

As far as the present model is concerned, in previous works we have obtained very good agreements between our estimates and the mature numerical calculations of exact geometries, as one can check in the family of systems depicted in Figs. 3 and 4 of Ref. [22]. The fact that the model represented so well such a variety of initial data and different mass ratios, motivated us to apply the same techniques to the case in which angular momentum was involved. However, since there are just two (still being refined) numerical calculations available to compare with, it is difficult to obtain much information at this stage.

As we have mentioned before our aim is to follow as close as possible the model used in [21] and [22]; however the fact that the initial conditions considered are relativistic poses several questions. For example, in matching the masses of the two stages we have used Eq. (48), so one might ask how would the results change if the relativistic γ factor was not used? This would certainly decrease the initial M and M_0 by about 13%; but E_N and E_{RT} would not change, so that the ration between the total energy radiated versus the changed M_0 would increase by the factor γ, that is about 15%.

Similarly, had we not used the relativistic correction on the angular momentum J, its initial value would have decreased by about 13%, but the relative variation shown in Fig. 2 would not have changed.

In any case, we think that by applying our model to these relativistic initial data, we are pushing the model to the boundary of is validity. Comparisons with future numerical simulations will shed light on this and indicate how far this model can be pushed.

The radiation of angular momentum seems to be negligible with these initial conditions. In order to consider higher values of the initial angular momentum, we would need to deal with other background geometries, as for example twisting algebraically special spacetimes. Regarding the smooth monotonic variation of it one can infer that, for these small initial angular momentum data, its behavior is driven by the exponential asymptotic behavior of the RT background geometry. There are not complicated initial variations in Ψ_1^0, that for example do appear in Ψ_4^0, as seen in Fig. 1.

When describing a concrete physical situation with these spacetimes, one is supposed to choose the gauge and fix the free functions in order to make the best representation of the system. It is somehow striking that the choice of the frame in first order has physical significance, and it is not pure gauge as one is accustomed to in the studies of linearized gravity around Minkowski spacetime.

ACKNOWLEDGMENTS

We acknowledge support from CONICET, SeCyT-UNC, NSF Grants No. PHY9900791 and PHY0090091, and Eberly Research Funds of Penn State. Some computations were performed in the VN cluster (vn.physics.ubc.ca) supported by the Canadian Foundation for Innovation.

[1] Luis Lehner, Class. Quantum Grav. **18**, R25 (2001).
[2] Steve Brandt *et al.*, Phys. Rev. Lett. **85**, 5496 (2000).
[3] Lawrence E. Kidder, Mark A. Scheel, and Saul A. Teukolsky, Phys. Rev. D **64**, 064017 (2001).
[4] Miguel Alcubierre, Bernd Brugmann, Denis Pollney, Edward Seidel, and Ryoji Takahashi, Phys. Rev. D **64**, 061501(R) (2001).
[5] H.J. Yo, T.W. Baumgarte, and S.L. Shapiro, Phys. Rev. D **64**, 124011 (2001).
[6] Bernard Kelly *et al.*, Phys. Rev. D **64**, 084013 (2001).
[7] R. Gomez, S. Husa, and J. Winicour, Phys. Rev. D **64**, 024010 (2001).
[8] L. Blanchet, Living Rev. Relativ. **5**, 3 (2002).
[9] C.M. Will, Prog. Theor. Phys. Suppl. **136**, 158 (1999).
[10] L. Blanchet, G. Faye, B. Iyer, and B. Joguet, Phys. Rev. D **65**, 061501(R) (2002).
[11] A. Buonanno and T. Damour, Phys. Rev. D **59**, 084006 (1999).
[12] K. Thorne, ‘‘Gravitational Radiation–A New Window Onto the Universe,’’ gr-qc/9704042.
[13] L. Grishchuk, V.M. Lipunov, K.A. Postnov, M.E. Prokhorov, and B.S. Sathyaprakash, Phys. Usp. **44**, 1 (2001).
[14] Richard H. Price and Jorge Pullin, Phys. Rev. Lett. **72**, 3297 (1994).
[15] J. Pullin, Prog. Theor. Phys. Suppl. **136**, 107 (1999).
[16] I. Robinson and R. Trautman, Proc. R. Soc. London **A265**, 463 (1962).
[17] K.P. Tod, Class. Quantum Grav. **6**, 1159 (1989).
[18] P.T. Chruściel and D.B. Singleton, Commun. Math. Phys. **147**, 137 (1992).
[19] L. Derry, R. Isaacson, and J. Winicour, Phys. Rev. **185**, 1647 (1969).
[20] O.M. Moreschi, Approximating vacuum asymptotic field equations around stationary spacetimes, GR16, Workshop A4, Durban, South Africa, 2001, oral presentation.
[21] O.M. Moreschi and S. Dain, Phys. Rev. D **53**, R1745 (1996).
[22] O.M. Moreschi, Phys. Rev. D **59**, 084018 (1999).
[23] Peter Anninos, David Hobill, Edward Seidel, Larry Smarr, and Wai-Mo Suen, Phys. Rev. D **52**, 2044 (1995).
[24] O.M. Moreschi and A. Perez, Class. Quantum Grav. **18**, 3701 (2001).
[25] E. Newman and R. Penrose, J. Math. Phys. **7**, 863 (1966).
[26] J.N. Goldberg *et al.*, J. Math. Phys. **8**, 2155 (1967).
[27] R. Penrose and W. Rindler, *Spinors and Space-Time* (Cambridge University Press, Cambridge, England, 1984), Vol. 1.
[28] R. Geroch, A. Held, and R. Penrose, J. Math. Phys. **14**, 874 (1973).
[29] S. Dain, O.M. Moreschi, and R.J. Gleiser, Class. Quantum Grav. **13**, 1155 (1996).
[30] D. Brill, Phys. Rev. **131**, 471 (1963).
[31] B. Bruegmann, Ann. Phys. (Leipzig) **9**, 227 (2000).
[32] B. Gustafsson, H.-O. Kreiss, and J. Oliger, *Time Dependent Problems and Difference Methods* (Wiley Interscience, New York, 1995).
[33] R. Gomez, L. Lehner, P. Papadopoulos, and J. Winicour, Class. Quantum Grav. **14**, 977 (1997).
[34] S. Teukolsky, Phys. Rev. D **61**, 087501 (2000).
[35] M. Alcubierre *et al.*, Phys. Rev. D **62**, 044034 (2000).
[36] O.M. Moreschi, Class. Quantum Grav. **3**, 503 (1986).
[37] O.M. Moreschi, Class. Quantum Grav. **5**, 423 (1988).
[38] O.M. Moreschi, Center of mass frame, angular momentum and asymptotic structure equations, GR16, Workshop A3, Durban, South Africa, 2001, oral presentation.
[39] R. Gleiser, G. Khanna, R. Price, and J. Pullin, New J. Phys. **2**, 3 (2000).
[40] W.G. Anderson, P. Brady, J. Creighton, and E. Flanagan, Phys. Rev. D **63**, 042003 (2001).
[41] J. Creighton, Phys. Rev. D **60**, 021101 (1999).